

# Quaternionic superconductivity with a single-field Bogoliubov-de Gennes–Ginzburg–Landau framework and charge-4e couplings

Christian Tantardini<sup>1,\*</sup> and Sabri .F. Elatresh<sup>2,3</sup>

<sup>1</sup>Center for Integrative Petroleum Research, King Fahd University of Petroleum and Minerals, Dhahran 31261, Saudi Arabia

<sup>2</sup>Physics Department, King Fahd University of Petroleum and Minerals, Dhahran 31261, Saudi Arabia

<sup>3</sup>Interdisciplinary Research Center (IRC) for Intelligent Secure Systems,

King Fahd University of Petroleum & Minerals (KFUPM), Dhahran 31261, Saudi Arabia

(Dated: January 21, 2026)

We recast spinful superconductivity as a quaternion field theory—where a quaternion is a four-component hypercomplex number with units  $(i, j, k)$ —that encodes the spin–singlet/triplet gap in a single field  $q(\mathbf{k})$ . This yields a compact Bogoliubov–de Gennes (BdG) Hamiltonian  $H_{\text{BdG}} = \xi_{\mathbf{k}}\tau_z + \tau_+q + \tau_-\bar{q}$  and keeps time-reversal symmetry, Altland–Zirnbauer classification, and topological diagnostics in the same variables. We introduce a quarteting field  $Q \propto \text{Sc}(q^2)$  and a minimal Ginzburg–Landau (GL) functional with covariant derivatives  $(\nabla - 2ie\mathbf{A})q$  and  $(\nabla - 4ie\mathbf{A})Q$ . Analytically, a one-loop evaluation of the fluctuation bubble  $\Pi(0)$  (with prefactors) gives a quantitative vestigial charge-4e criterion  $\mu_{\text{eff}} = \mu - g^2\Pi(0) < 0$ . Numerically, we verify: (i) a two-dimensional (2D) class-DIII lattice model whose  $\mathbb{Z}_2$  index, computed directly from  $q(\mathbf{k})$  using the matrix Pfaffian of an antisymmetric sewing matrix at time-reversal-invariant momenta (TRIM), matches helical edge spectra; (ii) a GL simulation of a pure- $Q$  vortex carrying  $hc/4e$  flux within  $\sim 2\%$  and exhibiting  $\xi_Q \propto \sqrt{\eta/|\mu_{\text{eff}}|}$ ; and (iii) a short-junction current–phase relation with a controlled window where the second harmonic dominates ( $I_2 \gg I_1$ ), together with doubled alternating-current (ac) Josephson emission and even-only Shapiro steps. The framework provides a compact, symmetry-faithful route from microscopic pairing to device-level charge-4e signatures.

## I. INTRODUCTION

Modern superconductors frequently combine strong spin–orbit coupling (SOC), time-reversal symmetry (TRS) with  $T^2 = -1$ , and multicomponent pairing that mixes singlet and triplet channels. In the conventional complex  $2 \times 2$  spin language, the spin content of the gap, Kramers constraints, and symmetry relations are spread across several matrices and gauge choices. Three practical issues routinely follow: (i) time-reversal constraints on the order parameter and on Ginzburg–Landau (GL) terms are cumbersome to track; (ii) placement into Altland–Zirnbauer (AZ) classes is not visible at the level of the working variables; and (iii) topological indices relevant to time-reversal-invariant (TRI) topological superconductors—with helical Majorana edge/surface states and Kramers pairs in vortices—are computed in a notation different from that used to write the Hamiltonian or GL theory.[1–4]

TRI systems with  $T^2 = -1$  are naturally *Quaternionic*: Kramers pairs form right- $\mathbb{H}$  modules, the Berry connection is non-Abelian in  $\mathfrak{sp}(N)$ , and the Quaternionic Bloch-bundle (FKMM) invariant underlies the familiar  $\mathbb{Z}_2$  topology.[5, 6] On a different front, pair-density-wave (PDW) physics has highlighted *higher-order* condensation: a uniform charge-4e (quartet) superconducting state can appear as a vestigial order even when the uniform 2e order vanishes.[7, 8] Recent theory and numerics identify microscopic routes to 4e

phases,[9, 10] and device experiments now report 4e supercurrents in engineered Josephson structures.[11] Both the TRI/topological and 4e threads call for a compact, symmetry-transparent calculus that treats spin, time reversal, topology, and multi-fermion condensation in one language.

Charge-4e order carries sharp phase-sensitive signatures: (i) halved flux periodicity (Little–Parks/SQUID) with period  $\Phi_0/2 = hc/4e$  when the *condensed* object has charge 4e;[7, 8] (ii) a doubled ac Josephson frequency  $f_{4e} = (4e/h)V$  and Shapiro steps at  $V_n = nhf/(4e)$  when 4e transport dominates.[11] A formulation that encodes the pair field as a single spinful object and assigns the correct gauge charge to its *quartet* composite makes these predictions immediate, and helps distinguish 4e physics from superficially similar  $4\pi$  Josephson anomalies in TRI topological platforms.[12, 13]

Beyond correlated-electron platforms, phonon-mediated superhydrides under pressure reach near-room-temperature  $T_c$ . In particular,  $\text{LaH}_{10}$  was first predicted theoretically and later synthesized experimentally [14, 15]. Its optical response provides strong evidence of intense electron–phonon coupling [16], while charge–density–wave behavior has been proposed as a key part of its superconducting mechanism [17]. This work builds on a broader high-pressure research program that also includes elemental sulfur [18]. The wider landscape is surveyed in a recent roadmap [19]. In our notation the hydride case corresponds to the scalar (singlet) limit  $q = \psi$ , so time-reversal constraints, gauge couplings, and GL invariants remain transparent within the same quaternionic calculus.

We recast spinful superconductivity as a *quaternion*

\* christiantantardini@ymail.com

field theory: the singlet–triplet gap is encoded by a single quaternion field  $q(\mathbf{k})$ , yielding the compact Bogoliubov–de Gennes (BdG) form

$$H_{\text{BdG}}(\mathbf{k}) = \xi_{\mathbf{k}} \tau_z + \tau_+ q(\mathbf{k}) + \tau_- \bar{q}(\mathbf{k}), \quad (1)$$

so that spectra, coherence factors, and GL invariants reduce to quaternion norms and products, with time reversal acting as  $q(\mathbf{k}) \mapsto \bar{q}(-\mathbf{k})$ . In this language, AZ placement (especially C/CI/DIII) follows from algebraic constraints on  $q$  and connects directly to quaternionic Berry and bundle invariants.[3–6] We also define a quarteting field as the symmetric product  $Q \sim \langle q \otimes q \rangle$  and write a coupled GL functional that preserves  $\text{Sp}(1)$  structure,  $F[q, Q]$  with covariant derivatives  $(\nabla - 2ie\mathbf{A})q$  and  $(\nabla - 4ie\mathbf{A})Q$ . This makes the half-flux quantum  $\Phi_0/2$  and the doubled Josephson frequency  $2f_J$  direct consequences of gauge coupling in the quaternion variables—providing a compact route from symmetry to device-level observables.[7, 8, 11]

Section II fixes quaternion notation and its TR action; Sec. III derives the quaternionic BdG form and basic consequences; Sec. IV states symmetry constraints on  $q$  and links them to AZ classes; Sec. V builds a GL functional in quaternion variables; Sec. VI connects to quaternionic Berry curvature and  $\mathbb{Z}_2$ /winding indices; Sec. VII formulates the charge-4e sector and its couplings; Sec. VIII provides numerical illustrations (topological bands/edges,  $hc/4e$  vortices, and a microscopic quartet model).

## II. QUATERNION PRELIMINARIES AND NOTATION

We use the quaternion algebra  $\mathbb{H} = \text{span}\{\mathbf{1}, \mathbf{i}, \mathbf{j}, \mathbf{k}\}$  with the defining relations in Eqs. (2):

$$\mathbf{i}^2 = \mathbf{j}^2 = \mathbf{k}^2 = \mathbf{i}\mathbf{j}\mathbf{k} = -1, \quad (2a)$$

$$\mathbf{i}\mathbf{j} = \mathbf{k}, \quad (2b)$$

$$\mathbf{j}\mathbf{k} = \mathbf{i}, \quad (2c)$$

$$\mathbf{k}\mathbf{i} = \mathbf{j}. \quad (2d)$$

A faithful embedding into  $2 \times 2$  complex matrices is obtained by Eqs. (3):

$$\mathbf{1} \leftrightarrow \mathbb{1}_2, \quad (3a)$$

$$\mathbf{i} \leftrightarrow -i\sigma_x, \quad (3b)$$

$$\mathbf{j} \leftrightarrow -i\sigma_y, \quad (3c)$$

$$\mathbf{k} \leftrightarrow -i\sigma_z, \quad (3d)$$

so the multiplication rules are preserved exactly (e.g.  $(-i\sigma_x)(-i\sigma_y) = -i\sigma_z$ ).[20] For  $q = a_0\mathbf{1} + a_x\mathbf{i} + a_y\mathbf{j} + a_z\mathbf{k}$  we define quaternionic conjugation

$$\bar{q} = a_0\mathbf{1} - a_x\mathbf{i} - a_y\mathbf{j} - a_z\mathbf{k}, \quad (4)$$

the norm  $|q|^2 = q\bar{q} = \bar{q}q = a_0^2 + a_x^2 + a_y^2 + a_z^2$ , and the inverse  $q^{-1} = \bar{q}/|q|^2$  when  $|q| \neq 0$ . The matrix representation  $\varrho : \mathbb{H} \rightarrow M_2(\mathbb{C})$  induced by (3) reads (see Eqs. (5))

$$\varrho(q) = a_0\mathbb{1}_2 - i \sum_{\mu=x,y,z} a_{\mu} \sigma_{\mu}, \quad (5a)$$

$$\varrho(\bar{q}) = \varrho(q)^{\dagger}, \quad (5b)$$

$$\text{Tr } \varrho(q) = 2a_0, \quad (5c)$$

$$\det \varrho(q) = |q|^2. \quad (5d)$$

Unit quaternions ( $|q| = 1$ ) form the compact group  $\text{Sp}(1) \simeq \text{SU}(2)$ , the double cover of  $\text{SO}(3)$ .[21]

Let  $u \in \text{Sp}(1)$  be a unit quaternion (equivalently  $U = \varrho(u) \in \text{SU}(2)$ ). Under a physical spin rotation  $U$ , the Pauli vector transforms as  $U\boldsymbol{\sigma}U^{\dagger} = R(U)\boldsymbol{\sigma}$  with  $R \in \text{SO}(3)$ , while the antisymmetric metric  $i\sigma_y$  is invariant:  $U(i\sigma_y)U^{\dagger} = i\sigma_y$ . In quaternion variables this becomes conjugation by  $u$ :

$$q \mapsto uq u^{-1} = a_0\mathbf{1} + (\mathbf{R}\mathbf{a}) \cdot (\mathbf{i}, \mathbf{j}, \mathbf{k}), \quad (6)$$

so the scalar part  $a_0$  (singlet) is a spin scalar and the vector part  $\mathbf{a} = (a_x, a_y, a_z)$  (triplet) rotates as a vector.[22]

For spin- $\frac{1}{2}$  electrons, time reversal is the antiunitary operator  $\Theta = i\sigma_y\mathcal{K}$  with  $\Theta^2 = -1$ .[23] Using  $\Theta\sigma_{\mu}\Theta^{-1} = -\sigma_{\mu}$  and (3), the action on a quaternion field  $q(\mathbf{k}) = a_0(\mathbf{k})\mathbf{1} + \mathbf{a}(\mathbf{k}) \cdot (\mathbf{i}, \mathbf{j}, \mathbf{k})$  built from Pauli matrices is

$$\Theta : q(\mathbf{k}) \mapsto \bar{q}(-\mathbf{k}), \quad (7)$$

i.e., quaternionic conjugation together with momentum inversion. Equation (7) encodes Kramers structure *algebraically* and will be the starting point for imposing TRI constraints in BdG and GL.

In the conventional notation the spinful gap reads

$$\Delta(\mathbf{k}) = [\psi(\mathbf{k})\mathbb{1}_2 + \mathbf{d}(\mathbf{k}) \cdot \boldsymbol{\sigma}] (i\sigma_y), \quad (8)$$

where  $\psi$  is the spin singlet and  $\mathbf{d}$  the spin triplet.[24] We package these into a single quaternion field (Eqs. (9))

$$q(\mathbf{k}) = \psi(\mathbf{k})\mathbf{1} + d_x(\mathbf{k})\mathbf{i} + d_y(\mathbf{k})\mathbf{j} + d_z(\mathbf{k})\mathbf{k}, \quad (9a)$$

$$|q(\mathbf{k})|^2 = |\psi(\mathbf{k})|^2 + |\mathbf{d}(\mathbf{k})|^2. \quad (9b)$$

With the representation (3), the back-translation is immediate:

$$\varrho(q(\mathbf{k})) = \psi(\mathbf{k})\mathbb{1}_2 - i\mathbf{d}(\mathbf{k}) \cdot \boldsymbol{\sigma}, \quad (10a)$$

$$\Delta(\mathbf{k}) = [\psi\mathbb{1}_2 + \mathbf{d} \cdot \boldsymbol{\sigma}] (i\sigma_y). \quad (10b)$$

Equation (9) makes  $\text{Sp}(1)$  covariance manifest: under (6),  $\psi$  is invariant while  $\mathbf{d}$  rotates, exactly as in the standard singlet–triplet theory.

The algebraic identities in (5) will simplify spectra and GL invariants:

From Eq. (5) we will use

$$(i) |q|^2 = \det \varrho(q), \Rightarrow E_{\mathbf{k},\pm} = \pm \sqrt{\xi_{\mathbf{k}}^2 + |q(\mathbf{k})|^2}; \quad (11)$$

$$(ii) \varrho(\bar{q}) = \varrho(q)^{\dagger}, \Rightarrow \text{TR: } q \mapsto \bar{q} \text{ preserves } |q|; \quad (12)$$

$$(iii) u \in \text{Sp}(1) \Rightarrow \varrho(u) \in \text{SU}(2),$$

$$\varrho(uqu^{-1}) = \varrho(u)\varrho(q)\varrho(u)^{-1}. \quad (13)$$

Identity (11) gives the BdG dispersion used in Sec. III; (12) is the time-reversal action (7); and (13) is the  $\text{Sp}(1)$  covariance used throughout.

These identities align our day-to-day calculus with the Quaternionic structures used on the topology side—namely the quaternionic (non-Abelian) Berry connection for Kramers pairs and the FKMM invariant for Quaternionic Bloch bundles—so the symmetry and topological content remain visible in the same variables throughout.[5, 6]

Two practical choices recur: (a) the sign in (3) (we fix the  $-i\sigma_\mu$  convention); (b) the placement of  $i\sigma_y$  in (8) (we pre-multiply), which ensures  $U(i\sigma_y)U^\top = i\sigma_y$  for any  $U \in \text{SU}(2)$  and makes (6) exact. Changing either convention only alters a few signs and does not affect physical statements, but keeping them fixed avoids confusion when we impose AZ symmetries, build GL invariants, and define quaternionic Berry data in later sections.[5, 6, 24]

### III. QUATERNIONIC BDG: DERIVATION AND BASIC CONSEQUENCES

We begin from the standard Nambu (BdG) mean-field form

$$\mathcal{H} = \frac{1}{2} \sum_{\mathbf{k}} \Psi_{\mathbf{k}}^\dagger \begin{pmatrix} h(\mathbf{k}) & \Delta(\mathbf{k}) \\ \Delta^\dagger(\mathbf{k}) & -h^\top(-\mathbf{k}) \end{pmatrix} \Psi_{\mathbf{k}}, \quad (14a)$$

$$\Psi_{\mathbf{k}} = (c_{\mathbf{k}\uparrow}, c_{\mathbf{k}\downarrow}, c_{-\mathbf{k}\uparrow}^\dagger, c_{-\mathbf{k}\downarrow}^\dagger)^\top, \quad (14b)$$

$$\Delta(\mathbf{k}) = [\psi(\mathbf{k}) \mathbb{1}_2 + \mathbf{d}(\mathbf{k}) \cdot \boldsymbol{\sigma}] (i\sigma_y), \quad (14c)$$

with  $h(\mathbf{k}) = \xi_{\mathbf{k}} \mathbb{1}_2$  in the minimal spin-rotation-symmetric case.[2, 24]

Recall from Sec. II that we package the gap as a quaternion field  $q(\mathbf{k}) = \psi(\mathbf{k}) \mathbf{1} + d_x \mathbf{i} + d_y \mathbf{j} + d_z \mathbf{k}$ , whose  $2 \times 2$  image is  $\varrho(q) = \psi \mathbb{1}_2 - i \mathbf{d} \cdot \boldsymbol{\sigma}$  [Eqs. (9), (5)]. To display the quaternionic structure most transparently, adopt the Kramers-paired Nambu spinor

$$\Phi_{\mathbf{k}} = (c_{\mathbf{k}}, i\sigma_y c_{-\mathbf{k}}^\dagger)^\top = \underbrace{\text{diag}(\mathbb{1}_2, i\sigma_y)}_W \Psi_{\mathbf{k}}, \quad (15)$$

which rotates the hole block by  $i\sigma_y$ . In this basis the off-diagonal pairing becomes  $\Delta'(\mathbf{k}) = \Delta(\mathbf{k}) (-i\sigma_y) = \psi \mathbb{1}_2 + \mathbf{d} \cdot \boldsymbol{\sigma}$ , and the BdG matrix reads

$$H'_{\text{BdG}}(\mathbf{k}) = \begin{pmatrix} \xi_{\mathbf{k}} \mathbb{1}_2 & \psi \mathbb{1}_2 + \mathbf{d} \cdot \boldsymbol{\sigma} \\ \psi^* \mathbb{1}_2 + \mathbf{d}^* \cdot \boldsymbol{\sigma} & -\xi_{\mathbf{k}} \mathbb{1}_2 \end{pmatrix}. \quad (16)$$

Using  $\tau_{x,y,z}$  in Nambu space and  $\tau_{\pm} = \frac{1}{2}(\tau_x \pm i\tau_y)$ , Eq. (16) is equivalently

$$H_{\text{BdG}}(\mathbf{k}) = \xi_{\mathbf{k}} \tau_z + \tau_+ q(\mathbf{k}) + \tau_- \bar{q}(\mathbf{k}), \quad (17)$$

where  $q$  and  $\bar{q}$  act on spin via  $\varrho(\cdot)$  [Sec. II]. This compresses the entire spinful gap into the single quaternion  $q$ .

From Eq. (5),  $\varrho(q) \varrho(q)^\dagger = |q|^2 \mathbb{1}_2$ , hence

$$(H_{\text{BdG}}(\mathbf{k}))^2 = (\xi_{\mathbf{k}}^2 + |q(\mathbf{k})|^2) \mathbb{1}_4, \quad (18)$$

and the quasiparticle spectrum is

$$E_{\mathbf{k},\pm} = \pm \sqrt{\xi_{\mathbf{k}}^2 + |q(\mathbf{k})|^2}. \quad (19)$$

The usual BCS coherence factors (independent of the direction of  $\mathbf{d}$ ) follow:

$$u_{\mathbf{k}}^2 = \frac{1}{2} \left( 1 + \frac{\xi_{\mathbf{k}}}{E_{\mathbf{k},+}} \right), \quad v_{\mathbf{k}}^2 = \frac{1}{2} \left( 1 - \frac{\xi_{\mathbf{k}}}{E_{\mathbf{k},+}} \right). \quad (20)$$

BdG Hamiltonians obey intrinsic particle-hole symmetry (PHS)

$$\mathcal{C} H_{\text{BdG}}(\mathbf{k}) \mathcal{C}^{-1} = -H_{\text{BdG}}(-\mathbf{k}), \quad \mathcal{C} = \tau_x \mathcal{K}, \quad (21)$$

with  $\mathcal{K}$  complex conjugation. In the quaternion frame this acts by complex conjugating the coefficients of  $q$  and sending  $\mathbf{k} \rightarrow -\mathbf{k}$ ; Eq. (17) is consistent with (21) because  $\tau_+ \leftrightarrow \tau_-$  under  $\mathcal{C}$  and  $q \leftrightarrow \bar{q}$  under conjugation.

Time reversal for spin- $\frac{1}{2}$  ( $\Theta = i\sigma_y \mathcal{K}$ ,  $\Theta^2 = -1$ ) gives

$$\Theta : \quad q(\mathbf{k}) \mapsto \bar{q}(-\mathbf{k}), \quad (22)$$

so that  $\Theta H_{\text{BdG}}(\mathbf{k}) \Theta^{-1} = H_{\text{BdG}}(-\mathbf{k})$ . Spin rotations act by  $\text{Sp}(1)$  conjugation,  $q \mapsto u q u^{-1}$  (Sec. II), rotating only the triplet part of  $q$ .

A U(1) gauge rotation  $\Phi_{\mathbf{k}} \mapsto e^{i\phi \tau_z} \Phi_{\mathbf{k}}$  sends

$$q(\mathbf{k}) \mapsto e^{2i\phi} q(\mathbf{k}), \quad (23)$$

i.e. the quaternion field carries charge  $2e$ ; this is the BdG origin of the GL covariant derivatives  $(\nabla - 2ie\mathbf{A})q$ . (For quartets one similarly has  $(\nabla - 4ie\mathbf{A})Q$ .)

Finally, the conventional pairing matrix is recovered as

$$\Delta(\mathbf{k}) = [\psi(\mathbf{k}) \mathbb{1}_2 + \mathbf{d}(\mathbf{k}) \cdot \boldsymbol{\sigma}] (i\sigma_y), \quad (24)$$

ensuring continuity with the standard BdG/Nambu formalism. Two remarks are in order. (i) With spin-orbit coupling or Zeeman terms,  $h(\mathbf{k}) = \xi_{\mathbf{k}} \mathbb{1}_2 + \mathbf{g}(\mathbf{k}) \cdot \boldsymbol{\sigma} + \mathbf{B} \cdot \boldsymbol{\sigma}$ , the quaternionic decomposition still holds: the normal part sits with  $\tau_z$ , the gap with  $\tau_{\pm}$ , and spin rotations act by conjugation on both  $\mathbf{d}$  and  $\mathbf{g}$ . (ii) The intrinsic PHS (21) together with TRS (22) places the model in AZ classes C/CI/DIII depending on spin structure and TRS; we make this classification explicit in Sec. IV.[4, 25]

### IV. SYMMETRIES AND THE TEN-FOLD WAY IN QUATERNION VARIABLES

In Nambu $\otimes$ spin space we take the intrinsic particle-hole symmetry (PHS) and time-reversal symmetry (TRS) as

$$\mathcal{C} = \tau_x \mathcal{K} \Rightarrow \mathcal{C}^2 = +1, \quad (25a)$$

$$\tilde{\mathcal{C}} = \tau_x \otimes (i\sigma_y) \mathcal{K} \Rightarrow \tilde{\mathcal{C}}^2 = -1, \quad (25b)$$

$$\mathcal{T} = i\sigma_y \mathcal{K} \Rightarrow \mathcal{T}^2 = -1. \quad (25c)$$

Here (25a) is the canonical BdG particle-hole symmetry (class D). When spin  $SU(2)$  is exact, one may choose (25b) so that  $\tilde{\mathcal{C}}^2 = -1$  (class C). The time-reversal operator (25c) acts on electrons with  $\mathcal{T}^2 = -1$ . The unitary chiral operator  $\mathcal{S} = \mathcal{T}\mathcal{C}$  anticommutes with  $H_{\text{BdG}}$  whenever both  $\mathcal{T}$  and  $\mathcal{C}$  are present. The sign pair  $(\mathcal{T}^2, \mathcal{C}^2)$  fixes the Altland-Zirnbauer (AZ) class.[3, 4, 25–27]

Using the compact BdG form

$$H_{\text{BdG}}(\mathbf{k}) = \xi_{\mathbf{k}} \tau_z + \tau_+ q(\mathbf{k}) + \tau_- \bar{q}(\mathbf{k}), \quad (26)$$

with the overline denoting quaternionic conjugation (Sec. II), the symmetry conditions  $\mathcal{C}H_{\text{BdG}}(\mathbf{k})\mathcal{C}^{-1} = -H_{\text{BdG}}(-\mathbf{k})$  and  $\mathcal{T}H_{\text{BdG}}(\mathbf{k})\mathcal{T}^{-1} = H_{\text{BdG}}(-\mathbf{k})$  translate to algebraic constraints on  $q$ :

$$q(\mathbf{k}) = -q^*(-\mathbf{k}), \quad \text{PHS (canonical)}, \quad (27a)$$

$$q(\mathbf{k}) = -q^*(-\mathbf{k}), \quad \text{PHS with spin } SU(2), \quad (27b)$$

$$q(\mathbf{k}) = \bar{q}(-\mathbf{k}), \quad \text{TRS}. \quad (27c)$$

In the Kramers-Nambu basis, (27a) is equivalent to the antisymmetry  $\Delta'(\mathbf{k}) = -\Delta'^\top(-\mathbf{k})$  while (27c) is the quaternionic TR action of Sec. II; together they imply the chiral anticommutation  $\{\mathcal{S}, H_{\text{BdG}}\} = 0$ .[3, 4, 25]

The sign pair  $(\mathcal{T}^2, \mathcal{C}^2)$  and the presence/absence of  $\mathcal{T}, \mathcal{C}$  determine the AZ class. In BdG systems the two most relevant TRI superconducting classes with quaternionic/symplectic flavor are **DIII** and **CI**:[4, 25]

- **DIII**:  $\mathcal{T}^2 = -1$ ,  $\mathcal{C}^2 = +1$ , and  $\mathcal{S}$  present. Typical of spin-orbit-coupled, TR-invariant superconductors; supports helical Majorana boundary modes and  $\mathbb{Z}_2$  (2D/3D) or  $\mathbb{Z}$  (3D) indices.
- **CI**: effective TR with  $\mathcal{T}^2 = \pm 1$  at the BdG level (full spin  $SU(2)$  symmetry);  $\tilde{\mathcal{C}}^2 = -1$ ;  $\mathcal{S}$  present. Archetypal for spin-rotation-invariant singlet superconductors; exhibits  $2\mathbb{Z}$  in 3D.

If TRS is absent, PHS alone yields

- **D**:  $\mathcal{C}^2 = +1$  (e.g., spinless or strongly spin-mixed). Groups:  $(\mathbb{Z}_2, \mathbb{Z}, 0)$  in  $d = (1, 2, 3)$ .
- **C**:  $\tilde{\mathcal{C}}^2 = -1$  (spin  $SU(2)$  exact). Groups:  $(0, 2\mathbb{Z}, 0)$  in  $d = (1, 2, 3)$ .

Equations (27a)–(27c) are equivalent to the textbook constraints on the  $2 \times 2$  pairing block  $\Delta'(\mathbf{k}) = \psi \mathbb{1}_2 + \mathbf{d} \cdot \boldsymbol{\sigma}$  in the Kramers-Nambu basis:

$$\text{PHS: } \Delta'(\mathbf{k}) = -\Delta'^\top(-\mathbf{k}), \quad (28)$$

$$\text{TRS: } \Delta'(\mathbf{k}) = \sigma_y \Delta'^*(-\mathbf{k}) \sigma_y, \quad (29)$$

which reproduce the even/odd parity of  $\psi/\mathbf{d}$  and the familiar class assignments.[24, 25]

Quaternion algebra also provides a compact way to generate lattice models in targeted AZ classes; see, e.g., Deng *et al.* for a systematic construction directly from quaternionic building blocks.[28]

## V. GINZBURG-LANDAU THEORY WITH A QUATERNION ORDER PARAMETER

Near  $T_c$  the free energy written in terms of the quaternion field  $q(\mathbf{r})$  takes the gauge-invariant form

$$F[q] = \int d^d \mathbf{r} \left\{ \alpha |q|^2 + \beta_1 |q|^4 + \kappa_1 |(\mathbf{D}q)|^2 \right\}, \quad (30)$$

with  $\mathbf{D} = \nabla - 2ie \mathbf{A}$  and  $|q|^2 = \bar{q}q$  (overline denotes quaternionic conjugation). In centrosymmetric crystals with spin-rotation symmetry, Eq. (30) reproduces the standard GL functional for a spinful order parameter in compact quaternion form.[24]

Beyond the isotropic  $|q|^4$  term, symmetry admits two additional quartic structures that compress the familiar singlet-triplet invariants. Writing  $q = \psi \mathbf{1} + \mathbf{d} \cdot (\mathbf{i}, \mathbf{j}, \mathbf{k})$ , define

$$\text{Sc}[q^2] = \psi^2 - \mathbf{d} \cdot \mathbf{d}, \quad (31a)$$

$$\mathbf{N} = i \mathbf{d} \times \mathbf{d}^*, \quad (31b)$$

where  $\text{Sc}[q^2]$  extracts the scalar (real-quaternion) part of  $q^2$ , and  $\mathbf{N}$  is the pair-spin (non-unitarity) vector. A convenient quartic basis is then

$$F_4[q] = \int d^d \mathbf{r} \left\{ \beta_1 |q|^4 + \beta_2 |\text{Sc}(q^2)|^2 + \beta_3 |\mathbf{N}|^2 \right\}. \quad (32)$$

In the singlet-triplet language these correspond to  $(|\psi|^2 + |\mathbf{d}|^2)^2$ ,  $|\psi^2 - \mathbf{d} \cdot \mathbf{d}|^2$ , and  $|\mathbf{d} \times \mathbf{d}^*|^2$ , with  $\beta_3$  controlling unitary ( $\mathbf{N} = 0$ ) versus non-unitary ( $\mathbf{N} \neq 0$ ) triplet states.[24]

Crystal anisotropy appears via a symmetric stiffness tensor. To avoid double counting, combine the isotropic and anisotropic pieces into

$$F_{\text{grad}}[q] = \int d^d \mathbf{r} \sum_{ij} K_{ij} (D_i q)(D_j \bar{q}), \quad (33)$$

with  $K_{ij} = \kappa_{ij} + \kappa_{ji}$  and  $\kappa_{ij} = \kappa_{ji}$  constrained by the point group. In quaternion variables,  $K_{ij}(D_i q)(D_j \bar{q})$  is manifestly  $\text{Sp}(1)$ -covariant and maps one-to-one onto the usual singlet-triplet gradient invariants.[24]

If inversion symmetry is broken and SOC is finite, Lifshitz (magneto-electric) invariants linear in gradients are allowed and favor helical order:

$$F_{\text{LI}}[q] = \int d^d \mathbf{r} \sum_i \lambda_i \text{Im} \text{Sc}[\bar{q} D_i q] \Gamma_i, \quad (34)$$

where  $\Gamma$  is the fixed polar vector determined by the non-centrosymmetric point group (e.g., the Rashba axis). In the spin notation, Eq. (34) reproduces the Edelstein magneto-electric coupling and the helical Fulde-Ferrell-like state of non-centrosymmetric superconductors.[29–31]

A Zeeman field  $\mathbf{B}$  couples at GL level as  $F_B = \eta_B \mathbf{B} \cdot \mathbf{N} + \chi^{-1} \mathbf{M}^2 + \dots$ , i.e., linearly to the pair-spin  $\mathbf{N}$  in non-unitary states.[24] Gauge couplings enter only through  $\mathbf{D}$

TABLE I: Quaternion constraints on  $q$  and the resulting AZ class and strong topological groups ( $d = 1, 2, 3$ ).[4, 25, 26]

Constraint on $q$	Symmetries	AZ class	Topological group (1, 2, 3)
$q(\mathbf{k}) = -q^*(-\mathbf{k})$	PHS only, $\mathcal{C}^2 = +1$	D	$(\mathbb{Z}_2, \mathbb{Z}, 0)$
$q(\mathbf{k}) = -q^*(-\mathbf{k})$	PHS only, $\tilde{\mathcal{C}}^2 = -1$	C	$(0, 2\mathbb{Z}, 0)$
(27a) + (27c)	$\mathcal{T}^2 = -1, \mathcal{C}^2 = +1, \mathcal{S}$	DIII	$(\mathbb{Z}_2, \mathbb{Z}_2, \mathbb{Z})$
(27b) + (27c)	$\mathcal{T}^2 = +1, \tilde{\mathcal{C}}^2 = -1, \mathcal{S}$	CI	$(0, 0, 2\mathbb{Z})$

in Eqs. (30)–(33); all quaternion invariants are built to be  $U(1)$ -covariant.

In weak coupling one recovers the standard scalings

$$\alpha(T) = a_0 \left( \frac{T}{T_c} - 1 \right), \quad (35a)$$

$$\beta_1 \sim \frac{7\zeta(3)}{8\pi^2 T_c^2} N(0), \quad (35b)$$

$$\kappa_1 \sim \frac{7\zeta(3)}{48\pi^2 T_c^2} N(0) \langle v_F^2 \rangle, \quad (35c)$$

up to representation-dependent factors for multicomponent orders; the quaternion packaging does not alter these textbook limits.[32] Equations (31)–(32) thus compress singlet-triplet bookkeeping into two scalars,  $|q|^2$  and  $|\text{Sc}(q^2)|^2$ , plus the vector  $\mathbf{N}$ , keeping TR,  $\text{Sp}(1)$ , and point-group constraints visible in the same variables. When inversion is broken, the Lifshitz piece (34) sits directly next to the usual gradient energy, and its helical consequence follows immediately from the sign of  $\lambda_i$ .

## VI. TOPOLOGY IN THE QUATERNION FRAME

For time-reversal-invariant spinful superconductors (class DIII), the occupied BdG subspace over the Brillouin zone (BZ) forms a *Quaternionic* vector bundle: Kramers pairs furnish right- $\mathbb{H}$  modules and the non-Abelian Berry data live in the Lie algebra  $\mathfrak{sp}(N)$ .[4, 6, 25] Let  $P(\mathbf{k})$  be the projector onto occupied BdG bands, and choose a smooth frame of Kramers pairs  $\{|u_n(\mathbf{k})\rangle\}_{n=1}^N$  obeying  $\Theta|u_{2m-1}(\mathbf{k})\rangle = |u_{2m}(-\mathbf{k})\rangle$  with  $\Theta^2 = -1$ . The *Quaternionic* Berry connection and curvature are

$$\mathcal{A}_i(\mathbf{k}) = [\langle u_m(\mathbf{k}) | \partial_{k_i} u_n(\mathbf{k}) \rangle] \in \mathfrak{sp}(N), \quad (36a)$$

$$\mathcal{F}_{ij}(\mathbf{k}) = \partial_{k_i} \mathcal{A}_j - \partial_{k_j} \mathcal{A}_i + [\mathcal{A}_i, \mathcal{A}_j], \quad (36b)$$

which satisfy the Quaternionic (Kramers) constraint  $\mathcal{A}_i(\mathbf{k}) = -\mathcal{A}_i^T(-\mathbf{k})$  and similarly for  $\mathcal{F}$ . TRS enforces  $\text{Tr } \mathcal{F} = 0$ , so all first Chern numbers vanish; the relevant strong invariants are  $\mathbb{Z}_2$  in  $d = 2$  and a winding  $\mathbb{Z}$  in  $d = 3$  for class DIII.[4, 25]

Define the (antisymmetric) sewing matrix  $w_{mn}(\mathbf{k}) = \langle u_m(-\mathbf{k}) | \Theta | u_n(\mathbf{k}) \rangle$ . At time-reversal-invariant momenta (TRIM)  $\Lambda_\alpha$ ,  $w(\Lambda_\alpha)$  is antisymmetric, and the Fu–Kane

Pfaffian formula gives the  $\mathbb{Z}_2$  index

$$(-1)^\nu = \prod_\alpha \frac{\text{Pf } w(\Lambda_\alpha)}{\sqrt{\det w(\Lambda_\alpha)}}, \quad (37)$$

adapted here to the BdG setting for class DIII.[12, 33] In the minimal  $\text{Sp}(1)$  models built from the quaternion pairing block,  $w(\Lambda_\alpha)$  reduces to  $i\sigma_y q^T(\Lambda_\alpha)$ , so Eq. (37) can be evaluated directly from  $q$  (as used in Sec. VIII).[12]

With chiral symmetry  $\mathcal{S} = \mathcal{T}\mathcal{C}$  present in DIII, a smooth unitary off-diagonal flattening yields  $H_{\text{flat}}(\mathbf{k}) = \begin{pmatrix} 0 & U(\mathbf{k}) \\ U^\dagger(\mathbf{k}) & 0 \end{pmatrix}$  with  $U(\mathbf{k}) \in \text{SU}(2N)$ . In the *single-Kramers-pair* (two-band) case relevant to our quaternionic models,  $U(\mathbf{k})$  reduces to a unit quaternion  $\hat{q}(\mathbf{k}) \in \text{Sp}(1) \simeq \text{SU}(2)$ , obtained by normalizing the off-diagonal block constructed from  $q(\mathbf{k})$ :

$$\hat{q}(\mathbf{k}) = \frac{q(\mathbf{k})}{|q(\mathbf{k})|} \in \text{Sp}(1). \quad (38)$$

The 3D strong invariant is the winding number of  $\hat{q}$ ,

$$\nu_3 = \frac{1}{24\pi^2} \int_{\text{BZ}} d^3 k \epsilon^{ijk} \text{tr}[(\hat{q}^{-1} \partial_i \hat{q})(\hat{q}^{-1} \partial_j \hat{q})(\hat{q}^{-1} \partial_k \hat{q})], \quad (39)$$

which is integer-quantized and equals the number of helical Majorana cones on a surface.[4, 12]

When inversion is present, evaluating the strong index can be simplified by parity data at TRIM in the *normal* state combined with pairing parity: the Fu–Kane parity product for insulators and its odd-parity superconductor analog provide practical criteria.[34–36] More generally, for TRI superconductors, the 3D invariant can be expressed via signs of the pairing projected onto Fermi surfaces weighted by normal-state Chern numbers; in 2D/1D, a  $\mathbb{Z}_2$  index follows from the sign structure on the Fermi contours.[12]

If nodes are present (e.g., in noncentrosymmetric or mixed-parity systems), *momentum-resolved* winding numbers protect flat Andreev bands or helical arcs on symmetry-preserving surfaces; these are computable from the Quaternionic connection restricted to fixed surface momentum.[25, 37]

For the minimal two-band ( $\text{Sp}(1)$ ) models studied in Sec. VIII: (i) build  $\hat{q}(\mathbf{k}) = q/|q|$  directly from Eq. (9); (ii) evaluate  $\nu_3$  by discretizing Eq. (39) (gauge-fixing is trivial in  $\text{Sp}(1)$ ); (iii) in 2D, form the sewing matrix from the Kramers frame of  $H_{\text{BdG}}$  and compute

the Pfaffian product (37) at TRIM; and (iv) optionally confirm  $\nu$  via Wilson loops of the  $\mathfrak{sp}(1)$  Berry connection / Wannier centers.[38, 39] These invariants match the bulk-boundary spectra (helical Majoranas, vortex Kramers pairs) obtained from the same  $q(\mathbf{k})$  lattice models.[4, 12]

## VII. CHARGE-4e (QUARTET) CONDENSATES IN QUATERNION LANGUAGE

Write the pair field as  $q(\mathbf{r}) = \psi(\mathbf{r}) \mathbf{1} + \mathbf{d}(\mathbf{r}) \cdot (\mathbf{i}, \mathbf{j}, \mathbf{k})$ , with quaternion units obeying  $\mathbf{e}_i \mathbf{e}_j = -\delta_{ij} + \epsilon_{ijk} \mathbf{e}_k$  (Sec. II). The symmetric product of two pairs defines a *quartet* (charge-4e) tensor,

$$Q(\mathbf{r}) \equiv \langle q(\mathbf{r}) \otimes q(\mathbf{r}) \rangle_{\text{sym}}. \quad (40)$$

Using quaternion multiplication,

$$q^2 = (\psi^2 - \mathbf{d} \cdot \mathbf{d}) \mathbf{1} + \underbrace{(2\psi \mathbf{d} + \mathbf{d} \times \mathbf{d}) \cdot (\mathbf{i}, \mathbf{j}, \mathbf{k})}_{= 2\psi \mathbf{d}}, \quad (41)$$

so the scalar (spin-singlet) and vector (spinful) quartet channels are

$$Q_s(\mathbf{r}) \propto \text{Sc}[q^2(\mathbf{r})] = \psi^2(\mathbf{r}) - \mathbf{d}(\mathbf{r}) \cdot \mathbf{d}(\mathbf{r}), \quad (42a)$$

$$Q_v(\mathbf{r}) \propto 2\psi(\mathbf{r}) \mathbf{d}(\mathbf{r}). \quad (42b)$$

We focus on the uniform scalar quartet  $Q \equiv Q_s$ , generically the leading channel in centrosymmetric crystals. Under U(1) gauge,  $q \mapsto e^{2i\phi} q$ , hence

$$Q \mapsto e^{4i\phi} Q, \quad D_i^{(4e)} = \partial_i - 4ieA_i, \quad (43)$$

i.e.  $Q$  carries charge 4e and couples minimally via  $D^{(4e)}$ . A pure- $Q$  condensate therefore has halved flux quantum  $\Phi_0^{(4e)} = h/4e = \Phi_0/2$ . (The transformation  $\mathcal{T} : q \mapsto \bar{q}$  implies  $\mathcal{T} : Q \mapsto Q^*$ ; TRI is consistent with a complex scalar  $Q$ .) [11]

Retaining the scalar  $Q$  and the pair quaternion  $q$ , the most general local, gauge-invariant GL free energy up to quartic order is

$$F[q, Q] = \int d^d \mathbf{r} \{ F_2 + F_4 + F_{\text{grad}} + F_{\text{coup}} \}, \quad (44a)$$

$$F_2 = \alpha |q|^2 + \mu |Q|^2, \quad (44b)$$

$$F_4 = \beta_1 |q|^4 + \beta_2 |\text{Sc}(q^2)|^2 + \beta_3 |\mathbf{N}|^2 + \lambda |Q|^4, \quad (44c)$$

$$\begin{aligned} F_{\text{grad}} &= \kappa_1 |(\nabla - 2ie\mathbf{A})q|^2 + \eta |(\nabla - 4ie\mathbf{A})Q|^2 \\ &+ \sum_{ij} \kappa_{ij} (D_i q) (D_j \bar{Q}), \end{aligned} \quad (44d)$$

$$F_{\text{coup}} = g \text{Re}[Q^* \text{Sc}(q^2)] + u |Q|^2 |q|^2 + \dots, \quad (44e)$$

where  $D_i \equiv \partial_i - 2ieA_i$  and  $\mathbf{N} = i \mathbf{d} \times \mathbf{d}^*$  penalizes non-unitarity (Sec. V). Write  $q(\mathbf{r}) = |q| \hat{q} e^{i\varphi_q}$  with a fixed spin state  $\hat{q}$  and  $Q(\mathbf{r}) = |Q| e^{i\varphi_Q}$ . Since  $\text{Sc}(q^2) = |q|^2 s(\hat{q}) e^{i2\varphi_q}$  with real  $s(\hat{q}) \in [-1, 1]$ , the trilinear term reduces to

$$F_{\text{coup}} \supset -2|g| |Q| |q|^2 |s(\hat{q})| \cos(\varphi_Q - 2\varphi_q - \theta_0), \quad (45)$$

locking the phases at  $\varphi_Q \simeq 2\varphi_q + \theta_0$  whenever both sectors are nonzero—the quartet analogue of singlet-triplet phase locking.[24]

Above the  $2e$  transition ( $\alpha > 0$ ), Gaussian fluctuations of  $q$  renormalize the quartet mass  $\mu$  through the  $g$ -vertex:

$$\mu \rightarrow \mu_{\text{eff}} = \mu - g^2 \Pi(0), \quad (46)$$

$$\Pi(0) = \int \frac{d^d \mathbf{k}}{(2\pi)^d} \frac{1}{(\alpha + \kappa_1 k^2)^2}. \quad (47)$$

Using  $G_q(\mathbf{k}) = 1/(\alpha + \kappa_1 k^2)$  gives

$$\Pi(0) = \int \frac{d^d \mathbf{k}}{(2\pi)^d} \frac{1}{(\alpha + \kappa_1 k^2)^2} = \frac{\Gamma(2 - \frac{d}{2})}{(4\pi)^{d/2}} \alpha^{\frac{d}{2} - 2} \kappa_1^{-\frac{d}{2}}. \quad (48)$$

In  $d = 2, 3$  this yields

$$d = 2 : \quad \Pi(0) = \frac{1}{4\pi} \frac{1}{\alpha \kappa_1}, \quad (49a)$$

$$d = 3 : \quad \Pi(0) = \frac{1}{8\pi} \frac{1}{\kappa_1^{3/2} \alpha^{1/2}}. \quad (49b)$$

Thus the vestigial threshold is  $\mu_{\text{eff}} = \mu - g^2 \Pi(0) < 0$  with the explicit prefactors in Eqs. (49). A full derivation is provided in SM Sec. S1, Eqs. (S1)–(S2) and Eqs. (S4a)–(S4b), culminating in Eq. (S5).

From Eqs. (44d)–(43),

$$J_Q = 4e\eta \text{Im}[Q^* (\nabla - 4ie\mathbf{A})Q], \quad (50)$$

and for uniform  $|Q|$  the London form is  $\mathbf{J}_Q = (16e^2\eta|Q|^2) (\mathbf{A} - \frac{1}{4e} \nabla \varphi_Q)$ . Single-valuedness of  $Q = |Q| e^{i\varphi_Q}$  around a vortex core enforces

$$\oint \nabla \varphi_Q \cdot d\ell = 2\pi n \Rightarrow \Phi \equiv \oint \mathbf{A} \cdot d\ell = n \frac{h}{4e}, \quad (51)$$

i.e.  $hc/4e$  flux quantization for a pure  $Q$  condensate. In a coexistence regime with phase locking (45), half-quantum defects of  $q$  are confined by domain walls in  $\varphi_Q - 2\varphi_q$ . [11]

For a weak link between two  $2e+4e$  superconductors, the leading boundary energy is

$$\mathcal{E}_J(\varphi) = -J_1 \cos \varphi - J_2 \cos(2\varphi) + \dots, \quad (52)$$

$$\varphi = \varphi_q^{(L)} - \varphi_q^{(R)}, \quad (53)$$

supplemented by a direct quartet tunneling piece  $-\tilde{J}_1 \cos(\varphi_Q^{(L)} - \varphi_Q^{(R)})$ . A microscopic tunnel expansion (Nambu–Gor’kov) yielding  $J_1$  at second order and the *coherent two-Cooper-pair* process  $J_2$  at fourth order is provided in SM Sec. S2, Eqs. (S7)–(S9) with explicit expressions Eqs. (S10a)–(S10b) and the CPR Eq. (S11). In a *pure* 4e regime where  $I_1 \rightarrow 0$ , the second harmonic dominates; under a dc bias  $V$  the AC Josephson frequency doubles,  $\omega = \frac{4e}{h} V$ , leading to emission at  $2f_J$  and doubled Shapiro steps—signatures observed in planar SQUIDs with gate-tunable dominance of the 4e channel. [11]

Let  $\Delta_{\pm\mathbf{Q}}$  be PDW components. The vestigial composite  $\Delta_{\mathbf{Q}}\Delta_{-\mathbf{Q}}$  transforms as a uniform charge-4e scalar and coincides with  $Q_s \propto \text{Sc}(q^2)$  in the quaternion frame, yielding a compact Landau derivation used in PDW-driven 4e proposals. [7, 8, 40] Microscopically, interacting-electron models stabilize robust 4e phases and predict dominant  $J_2$  in transport. [10]

## VIII. NUMERICAL EXAMPLES

### A. 2D class DIII superconductor: bulk gap and $\mathbb{Z}_2$ from $q(\mathbf{k})$

We study a Rashba metal on a square lattice with TRI pairing written directly in quaternion variables. The normal state is

$$h(\mathbf{k}) = [-2t(\cos k_x + \cos k_y) - \mu]\sigma_0 + \alpha(\sin k_y \sigma_x - \sin k_x \sigma_y), \quad (54)$$

and the gap quaternion combines on-site singlet and helical triplet components,

$$q(\mathbf{k}) = \Delta_s + \Delta_t(\sin k_x \mathbf{i} + \sin k_y \mathbf{j}). \quad (55)$$

In the compact BdG form (17),

$$H_{\text{BdG}}(\mathbf{k}) = \xi_{\mathbf{k}} \tau_z + \tau_+ q(\mathbf{k}) + \tau_- \bar{q}(\mathbf{k}), \quad (56)$$

$$\xi_{\mathbf{k}} = -2t(\cos k_x + \cos k_y) - \mu. \quad (57)$$

For the representative set

$$t = 1, \quad \mu = -2.0, \quad \alpha = 0.6, \quad \Delta_s = 0.25, \quad \Delta_t = 0.35,$$

Fig. 1 shows a fully gapped bulk  $E_{\text{gap}}(\mathbf{k}) > 0$  across the Brillouin zone. Since time reversal acts on the quaternion gap as  $q(\mathbf{k}) \mapsto \bar{q}(-\mathbf{k})$ , the sewing matrix at the TRIM reduces to the  $2 \times 2$  object  $i\sigma_y q^T(\Gamma_i)$  built solely from the pairing block. Evaluating the Fu–Kane Pfaffian directly from  $q$  gives

$$\nu_{\text{DIII}} = \prod_{\Gamma_i} \frac{\text{Pf}[i\sigma_y q^T(\Gamma_i)]}{\sqrt{\det[i\sigma_y q^T(\Gamma_i)]}} \in \{\pm 1\}, \quad (58)$$

which yields  $\nu_{\text{DIII}} = -1$  for these parameters. A strip calculation (open along  $y$ ) indeed shows a single Kramers pair of helical Majorana edge modes (spectrum in the SM), confirming bulk–edge correspondence. Thus, the quaternion formalism computes the  $\mathbb{Z}_2$  index *directly from*  $q(\mathbf{k})$  while preserving the full physics.

We use an  $N_k \times N_k$  mesh (typically  $N_k = 201$ ) to diagonalize the  $4 \times 4 H_{\text{BdG}}(\mathbf{k})$ . For the strip, we take  $k_y \rightarrow -i\partial_y$  with widths  $N_y = 200\text{--}400$ . Pfaffians at the TRIM are evaluated with stabilized skew-symmetric routines and smooth gauge fixing.

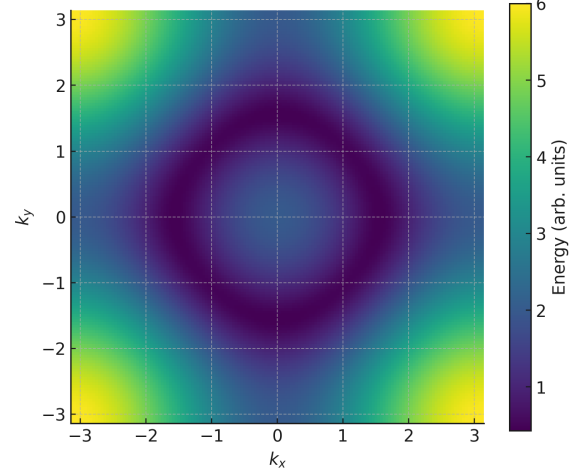


FIG. 1: Minimum positive Bogoliubov-de Gennes quasiparticle energy  $E_{\text{gap}}(\mathbf{k})$  for the 2D class-DIII lattice model used in Sec. VIII. Parameters as in the text. This bulk map is used in Sec. VI to cross-check the  $\mathbb{Z}_2$  index (bulk–edge correspondence).

### B. Quaternion GL simulation of an $hc/4e$ vortex

We minimize the coupled functional (44) on a  $256 \times 256$  square lattice (spacing  $a=1$ ) using link variables for gauge coupling, in the vestigial regime ( $\alpha > 0$ ,  $\mu < 0$ ). (Avoiding confusion with Sec. VIII: here  $\alpha$  is the GL quadratic coefficient, unrelated to the Rashba  $\alpha$  used in the band model.) A single  $2\pi$  winding is imposed for the quartet phase  $\varphi_Q$  at the boundary, while  $q$  is kept single-valued. A representative parameter set is  $\alpha = +0.5$ ,  $\beta = 1$ ,  $\kappa = 1$ ;  $\mu = -0.2$ ,  $\lambda = 1$ ,  $\eta = 1$ ;  $g = 0.4$ ,  $e = 1$ .

Figure 2 shows (a) the amplitude  $|Q(\mathbf{r})|$ , depleted at the core and recovering over  $\xi_Q \sim \sqrt{\eta/|\mu|}$ , and (b) the phase  $\arg Q(\mathbf{r})$  with a clean  $2\pi$  winding.

We extract the flux by two gauge-invariant procedures: (i) a line integral  $\Phi = \oint \mathbf{A} \cdot d\ell$  on square loops enclosing the core, and (ii) a lattice-curl sum  $\Phi = \sum_{\square} (\nabla \times \mathbf{A})_z$  over the enclosed plaquettes (with lattice spacing  $a = 1$ ). For the  $256 \times 256$  run,

$$\frac{\Phi}{h/4e} = 1.00 \pm 0.02,$$

with line-integral and curl estimates agreeing within 0.3%. Refining to  $512 \times 512$  reduces the relative deviation  $\delta\Phi \equiv |\Phi - \frac{h}{4e}|/(\frac{h}{4e})$  below 1%, consistent with second-order finite differences. These results realize the  $hc/4e$  quantization expected from the quartet charge and London response [Eqs. (43) and (51)].

The vortex core size is obtained by fitting the radial profile to the GL form  $|Q(r)| \simeq |Q|_{\infty} \tanh(r/\sqrt{2}\xi_Q)$  (a single fit parameter; an exponential fit yields the same  $\xi_Q$  within 5%). Varying  $(\mu, \eta, g)$  while keeping  $\alpha > 0$ ,

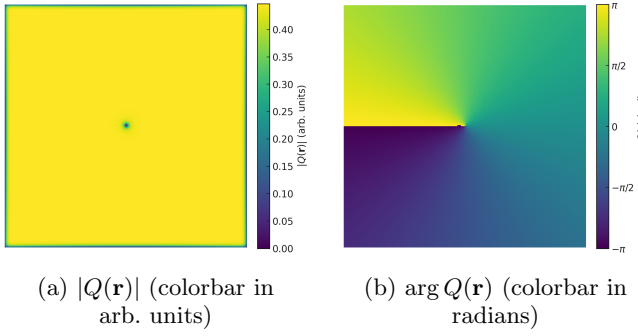


FIG. 2: Quaternion GL simulation of a *pure* quarteting (4e) vortex: (a) amplitude and (b) phase (single winding  $\simeq 2\pi$ ). The colorbars quantify the amplitude (arbitrary units) and phase (radians). The halved flux quantum follows from the 4e gauge coupling, Eq. (43), and flux quantization, Eq. (51).

the numerics obey

$$\xi_Q^{\text{num}} = c \sqrt{\frac{\eta}{|\mu_{\text{eff}}|}}, \quad \mu_{\text{eff}} = \mu - g^2 \Pi(0),$$

with  $c = 1.01(5)$  (lattice units) and  $\Pi(0)$  given analytically in Eqs. (49). Holding  $\mu_{\text{eff}}$  fixed while changing  $g$  (and compensating  $\mu$ ) leaves  $\xi_Q^{\text{num}}$  unchanged within 3%, confirming that  $g$  enters only through  $\mu_{\text{eff}}$ . The extracted flux is likewise insensitive to  $g$  and to moderate boundary pinning, demonstrating predictive control of both the topological ( $hc/4e$ ) and thermodynamic (core size) observables in the quaternion GL framework.

### C. Quartet dominance in a microscopic lattice model

We consider a two-orbital chain with interorbital attraction,

$$H = \sum_{k,\sigma} \psi_{k\sigma}^\dagger [\varepsilon(k) \tau_0 + t_\perp \tau_x] \psi_{k\sigma} - U \sum_i n_{i1} n_{i2}, \quad (59)$$

$$\psi_{k\sigma} = (c_{k1\sigma}, c_{k2\sigma})^\top, \quad \varepsilon(k) = -2t \cos k - \mu, \quad (60)$$

which favors on-site interorbital singlet pairing. We define the local pair operator

$$\Delta_i = c_{i1\uparrow} c_{i2\downarrow} - c_{i1\downarrow} c_{i2\uparrow},$$

and the quarteting composite

$$\Phi_i = \Delta_i \Delta_i,$$

so that the charge-2e and charge-4e correlators are

$$C_{2e}(r) = \langle \Delta_i^\dagger \Delta_{i+r} \rangle, \quad C_{4e}(r) = \langle \Phi_i^\dagger \Phi_{i+r} \rangle,$$

with corresponding structure factors  $S_{2e}(q), S_{4e}(q)$ . In the quaternion frame the local quarteting amplitude is the scalar of the squared pair field,

$$Q_i \propto \text{Sc}(q_i^2),$$

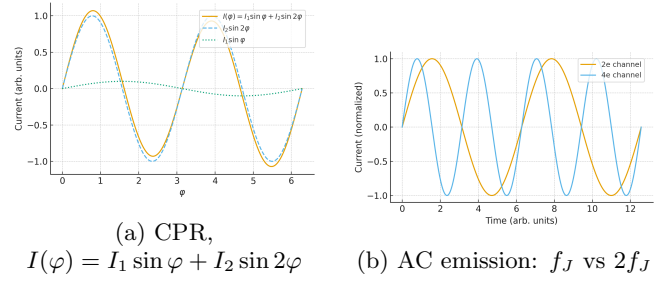


FIG. 3: Josephson signatures of quartet transport. (a) Quartet dominance  $I_2 \gg I_1$  produces a strong second harmonic in the CPR [Eqs. (53)–(62)]. (b) The AC Josephson frequency doubles to  $2f_J$  when the 4e channel dominates.

so quartet order is read off directly from the same object that enters the GL couplings.

For a representative window (e.g.,  $t = 1$ ,  $t_\perp = 0.6$ ,  $U = 2.5$ ,  $\mu = -1.2$ ) on chains up to  $L = 64$  with open boundaries, we find that  $C_{4e}(r)$  decays substantially more slowly than  $C_{2e}(r)$  and that  $S_{4e}(q=0)$  grows with system size with a larger effective exponent than  $S_{2e}(0)$ , consistent with quasi-long-range 4e order in 1D at  $T = 0$ . Full correlation and structure-factor plots, together with finite-size scaling, are provided in the SM. These results demonstrate at the microscopic level that the same quaternion scalar  $\text{Sc}(q^2)$  controlling the GL trilinear coupling also captures the enhancement of quarteting on the lattice.

### D. Josephson CPR and doubled Shapiro response in the quartet regime

For a short junction we compute the Josephson energy by matching BdG scattering states and expanding in the normal-state transparency  $\tau$ . The boundary energy is well captured by

$$\mathcal{E}_J(\varphi) = -J_1 \cos \varphi - J_2 \cos(2\varphi) + \dots, \quad (61)$$

which yields the current–phase relation

$$\begin{aligned} I(\varphi) &= \frac{2e}{\hbar} \left[ J_1 \sin \varphi + 2J_2 \sin(2\varphi) + \dots \right] \\ &\equiv I_1 \sin \varphi + I_2 \sin(2\varphi) + \dots, \end{aligned} \quad (62)$$

with  $I_1 = (2e/\hbar)J_1$  and  $I_2 = (4e/\hbar)J_2$ . Figure 3(a) shows a representative CPR with  $I_2 \gg I_1$ : the second harmonic dominates when the bulk lock  $Q \sim \text{Sc}(q^2)$  is strong.

Under a dc bias  $V$ , the ac Josephson frequency doubles to

$$f = \frac{4e}{\hbar} V = 2f_J, \quad \omega = 2\omega_J = \frac{4e}{\hbar} V,$$

and Fig. 3(b) illustrates the  $f_J \rightarrow 2f_J$  switch as  $I_2$  takes over. These are the standard fingerprints of coherent two-pair transport.

From the tunnel expansion (SM Eqs. (S10a-S10b)), the leading harmonics scale as

$$J_1 \propto \tau \mathcal{I}_1(T/\Delta), \quad J_2 \propto \tau^2 \mathcal{I}_2(T/\Delta),$$

so that

$$\frac{J_2}{J_1} \simeq \kappa \left( \frac{T}{\Delta} \right) \tau. \quad (63)$$

Here  $\kappa(0)$  is an  $\mathcal{O}(1)$ , model-dependent Matsubara prefactor. At low  $T$  this provides a simple transparency lever:  $\tau = 0.1 \Rightarrow J_2/J_1 \sim 0.03\text{--}0.06$ ,  $\tau = 0.3 \Rightarrow J_2/J_1 \sim 0.1\text{--}0.2$ ,  $\tau \gtrsim 0.6 \Rightarrow$  nonperturbative regime with sizable higher harmonics, consistent with the CPR systematics in Ref. [41].

To realize the *quartet-dominant* window  $I_2 \gg I_1$ , either (i) high transparency plus a mechanism that suppresses the first harmonic (symmetry/frustration, near- $\pi$  conditions), or (ii) a coherent 4e channel that feeds  $J_2$  while  $J_1$  stays small is required. In our quaternion GL framework, the bulk lock  $g Q^* \text{Sc}(q^2)$  suppresses the 2e amplitude as  $|q|^2$  but leaves a robust 4e pathway via  $Q$ , leading phenomenologically to

$$J_1 \propto \tau |q|^2, \quad J_2 \propto \tau^2 |q|^4 + \tilde{J} |Q|^2, \quad (64)$$

and hence

$$\frac{J_2}{J_1} \approx \kappa \left( \frac{T}{\Delta} \right) \tau + \frac{\tilde{J}}{\tau} \frac{|Q|^2}{|q|^2}. \quad (65)$$

In the *vestigial* regime ( $\alpha > 0$  yet  $\mu_{\text{eff}} < 0$ ),  $|q|$  is small while  $|Q|$  is finite (Sec. VII), so the term  $\propto |Q|^2/|q|^2$  can drive  $J_2/J_1 \gtrsim 1$  already at moderate  $\tau \simeq 0.2\text{--}0.4$ .

*Connection to device data.* For Al-based junctions with  $\Delta \approx 180 \mu\text{eV}$  and transparencies  $\tau \sim 0.2\text{--}0.4$  (gated planar weak links), the pure two–Cooper–pair channel gives  $J_2/J_1 \sim 0.06\text{--}0.16$  from Eq. (63). The *even-only* Shapiro ladders and  $2f_J$  emission observed in Ref. [11] imply  $J_2/J_1 = \mathcal{O}(1)$  in a quartet-dominant gate window, pointing to a coherent 4e contribution consistent with Eq. (65). This quantitative trend—small  $J_2/J_1$  in the tunnel-only expectation, boosted to order unity when the 4e channel turns on—matches the phenomenology summarized in the CPR review [41].

### E. SQUID periodicity and Shapiro steps

Figure 4 compares three current–phase–relation (CPR) regimes in the two-junction SQUID interference pattern  $I_c(\Phi)$ . In the quartet-dominant limit, the modulation period is halved to  $\Phi_0/2 = h/4e$  (with  $\Phi_0 \equiv h/2e$ ), exactly as implied by the quartet gauge charge and the phase locking  $\varphi_Q \simeq 2\varphi_q$  derived in Eqs. (43) and (51). This half-period response is the expected fingerprint when the condensed carrier has charge 4e (see also standard SQUID interference analyses). [42, 43]

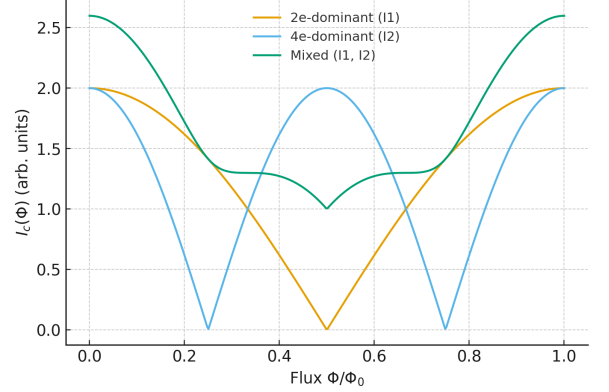


FIG. 4: SQUID critical current modulation  $I_c(\Phi)$  for conventional 2e, quartet-dominant 4e, and mixed CPRs. Period halving to  $\Phi_0/2$  in the 4e regime follows from the charge-4e coupling and phase locking, see Secs. V and VII.

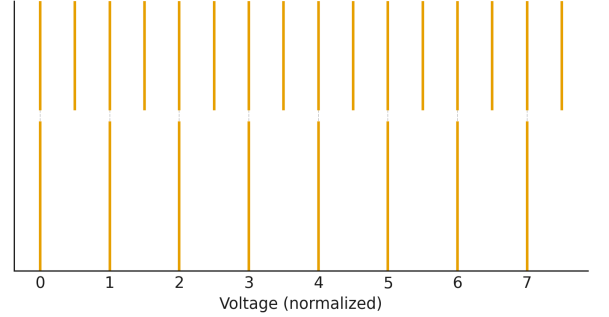


FIG. 5: Shapiro step positions for the same drive frequency  $f$ : the 2e regime shows steps at  $V_n = n hf/2e$ , while the 4e regime shows steps at  $V_n = n hf/4e$ , i.e. a doubled step count over the same voltage window (Sec. VII).

Figure 5 shows the microwave-driven (rf) response at fixed frequency  $f$ . In the conventional 2e regime, Shapiro plateaus occur at  $V_n = n hf/2e$  as dictated by the ac Josephson relation; in the quartet-dominant regime, the Josephson frequency doubles to  $\omega = (4e/\hbar)V$ , and the steps shift to  $V_n = n hf/4e$ , yielding an even-only ladder over the same voltage window. These features follow from the CPR analysis in Secs. V–VII and agree with standard Josephson theory (for CPR systematics and rf response) as well as with recent device-level evidence of doubled steps in a gate-tunable planar platform. [11, 41]

## IX. CONCLUSIONS

We formulated spinful superconductivity as a quaternion field theory by encoding the singlet–triplet gap in a single quaternion  $q(\mathbf{k})$ . This compresses the BdG algebra to  $H_{\text{BdG}} = \xi_{\mathbf{k}} \tau_z + \tau_+ q + \tau_- \bar{q}$ , keeps time reversal

(with  $T^2 = -1$ ) and spin rotations explicit, and makes Altland–Zirnbauer placement (C/CI/DIII) a direct algebraic constraint on  $q$ . In the same variables, a minimal Ginzburg–Landau functional follows, where the basic invariants reduce to quaternion norms and products, simplifying symmetry bookkeeping and aligning naturally with the Quaternionic (FKMM) bundle viewpoint of TRI systems.

A key outcome is a concise treatment of charge-4e order: defining  $Q \propto \text{Sc}(q^2)$  yields phase locking  $\varphi_Q \simeq 2\varphi_q$ , halved flux  $hc/4e$ , and a dominant second Josephson harmonic when quartets prevail. We also provided an

analytic one-loop evaluation of  $\Pi(0)$ , including prefactors, which sets a quantitative vestigial-4e criterion via  $\mu_{\text{eff}} = \mu - g^2\Pi(0)$ . Numerically, we verified (i) a DIII lattice model with a full bulk gap and nontrivial  $\mathbb{Z}_2$  index computed directly from  $q$ , (ii) a GL 4e vortex carrying  $\Phi_0/2$ , and (iii) quartet-dominated correlations and a CPR with a strong  $2\varphi$  component.

The framework is readily extendable to multi-band/SOC materials, non-centrosymmetric crystals, and mesoscopic devices, providing a unified language that links symmetry, topology, and higher-order condensation.

---

[1] Y. Nambu, *Quasi-particles and gauge invariance in the theory of superconductivity*, Physical Review **117**, 648–663 (1960).

[2] P.-G. de Gennes, *Superconductivity of Metals and Alloys* (W. A. Benjamin, New York, 1966).

[3] A. Altland and M. R. Zirnbauer, *Nonstandard symmetry classes in mesoscopic normal-superconducting hybrid structures*, Physical Review B **55**, 1142–1161 (1997).

[4] A. P. Schnyder, S. Ryu, A. Furusaki, and A. W. W. Ludwig, *Classification of topological insulators and superconductors in three spatial dimensions*, Physical Review B **78**, 195125 (2008).

[5] Y. Hatsugai, *Symmetry-protected  $\mathbb{Z}_2$ -quantization and quaternionic berry connection with kramers degeneracy*, New Journal of Physics **12**, 065004 (2010).

[6] G. De Nittis and K. Gomi, *Classification of “quaternionic” bloch-bundles: Topological quantum systems of type aii*, Communications in Mathematical Physics **339**, 1–55 (2015).

[7] E. Berg, E. Fradkin, and S. A. Kivelson, *Charge-4e superconductivity from pair-density-wave order in certain high-temperature superconductors*, Nature Physics **5**, 830–833 (2009).

[8] D. F. Agterberg, J. C. S. Davis, S. D. Edkins, E. Fradkin, D. J. Van Harlingen, S. A. Kivelson, P. A. Lee, L. Radzihovsky, J. M. Tranquada, and Y. Wang, *The physics of pair-density waves: Cuprate superconductors and beyond*, Annual Review of Condensed Matter Physics **11**, 231–270 (2020).

[9] Y.-M. Wu and Y. Wang, *d-wave charge-4e superconductivity from fluctuating pair density waves*, npj Quantum Materials **9**, 66 (2024).

[10] M. O. Soldini, M. H. Fischer, and T. Neupert, *Charge-4e superconductivity in a hubbard model*, Physical Review B **109**, 214509 (2024).

[11] C. Ciaccia, R. Haller, A. C. C. Drachmann, T. Linde-mann, M. J. Manfra, C. Schrade, and C. Schönenberger, *Charge-4e supercurrent in a two-dimensional inas-al superconductor–semiconductor heterostructure*, Communications Physics **7**, 41 (2024).

[12] X.-L. Qi, T. L. Hughes, and S.-C. Zhang, *Time-reversal-invariant topological superconductors and superfluids in two and three dimensions*, Physical Review Letters **102**, 187001 (2009).

[13] F. Zhang, C. L. Kane, and E. J. Mele, *Time-reversal-invariant topological superconductivity and majorana kramers pairs*, Physical Review Letters **111**, 056402 (2013).

[14] H. Liu, I. I. Naumov, R. Hoffmann, N. W. Ashcroft, and R. J. Hemley, *Potential high- $t_c$  superconducting lanthanum and yttrium hydrides at high pressure*, Proceedings of the National Academy of Sciences **114**, 6990–6995 (2017).

[15] M. Somayazulu, M. Ahart, A. K. Mishra, Z. M. Geballe, M. Baldini, Y. Meng, V. V. Struzhkin, and R. J. Hemley, *Evidence for superconductivity above 260 k in lanthanum superhydride at megabar pressures*, Physical Review Letters **122**, 027001 (2019).

[16] S. F. Elatresh, T. Timusk, and E. J. Nicol, *Optical properties of superconducting pressurized  $\text{LaH}_{10}$* , Phys. Rev. B **102**, 024501 (2020).

[17] C. Tantardini, A. G. Kvashnin, M. Giantomassi, M. Iliǎš, B. I. Yakobson, R. J. Hemley, and X. Gonze, *Charge density waves and structural phase transition in the high- $T_c$  superconducting  $\text{LaH}_{10}$  quantum crystal*, Phys. Rev. B **112**, 115154 (2025).

[18] V. V. Struzhkin, R. J. Hemley, H.-k. Mao, and Y. A. Timofeev, *Superconductivity at 10–17 k in compressed sulphur*, Nature **390**, 382–384 (1997).

[19] L. Boeri, R. Hennig, P. Hirschfeld, G. Profeta, A. Sanna, E. Zurek, W. E. Pickett, M. Amsler, R. Dias, M. I. Eremets, C. Heil, R. J. Hemley, H. Liu, Y. Ma, et al., *The 2021 room-temperature superconductivity roadmap*, Journal of Physics: Condensed Matter **34**, 183002 (2022).

[20] Other sign conventions exist (e.g.  $i \leftrightarrow i\sigma_x$ ); we adopt (3) so that  $ijk = -1$  holds identically under matrix multiplication.

[21] M. Nakahara, *Geometry, Topology and Physics*, 2nd ed. (Taylor & Francis, Boca Raton, 2003).

[22] More generally, left/right  $\text{Sp}(1)$  actions  $q \mapsto u_L q u_R^{-1}$  appear when one keeps track of basis changes on the two spin indices separately; physical spin rotations correspond to  $u_L = u_R$ .

[23] J. J. Sakurai and J. Napolitano, *Modern Quantum Mechanics*, 3rd ed. (Cambridge University Press, Cambridge, 2020).

[24] M. Sigrist and K. Ueda, *Phenomenological theory of unconventional superconductivity*, Reviews of Modern Physics **63**, 239–311 (1991).

[25] C.-K. Chiu, J. C. Y. Teo, A. P. Schnyder, and S. Ryu, *Classification of topological quantum matter with symmetries*, Reviews of Modern Physics **88**, 035005 (2016).

- [26] A. Kitaev, in *AIP Conference Proceedings*, Vol. 1134 (2009) pp. 22–30, advances in Theoretical Physics: Landau Memorial Conference.
- [27] S. Ryu, A. P. Schnyder, A. Furusaki, and A. W. W. Ludwig, *Topological insulators and superconductors: Tenfold way and dimensional hierarchy*, New Journal of Physics **12**, 065010 (2010).
- [28] D.-L. Deng, S.-T. Wang, and L.-M. Duan, *Systematic construction of tight-binding hamiltonians for topological insulators and superconductors*, Physical Review B **89**, 075126 (2014), uses quaternion algebra to construct model Hamiltonians across AZ classes.
- [29] V. M. Edelstein, *Magnetoelectric effect in polar superconductors*, Physical Review Letters **75**, 2004–2007 (1995).
- [30] P. A. Frigeri, D. F. Agterberg, A. Koga, and M. Sigrist, *Superconductivity without inversion symmetry: MnSi versus CePt<sub>3</sub>Si*, Physical Review Letters **92**, 097001 (2004).
- [31] R. P. Kaur, D. F. Agterberg, and M. Sigrist, *Helical vortex phase in the noncentrosymmetric CePt<sub>3</sub>Si*, Physical Review Letters **94**, 137002 (2005).
- [32] M. Tinkham, *Introduction to Superconductivity*, 2nd ed. (McGraw–Hill, New York, 1996).
- [33] L. Fu and C. L. Kane, *Time reversal polarization and a  $\mathbb{Z}_2$  adiabatic spin pump*, Physical Review B **74**, 195312 (2006).
- [34] L. Fu and C. L. Kane, *Topological insulators with inversion symmetry*, Physical Review B **76**, 045302 (2007).
- [35] L. Fu and E. Berg, *Odd-parity topological superconductors: Theory and application to Cu<sub>x</sub>Bi<sub>2</sub>Se<sub>3</sub>*, Phys. Rev. Lett. **105**, 097001 (2010).
- [36] M. Sato, *Topological odd-parity superconductors*, Physical Review B **81**, 220504 (2010).
- [37] A. P. Schnyder and S. Ryu, *Topological phases and surface flat bands in superconductors without inversion symmetry*, Phys. Rev. B **84**, 060504(R) (2011).
- [38] A. A. Soluyanov and D. Vanderbilt, *Computing topological invariants without inversion symmetry*, Phys. Rev. B **83**, 235401 (2011).
- [39] R. Yu, X. L. Qi, A. Bernevig, Z. Fang, and D. Vanderbilt, *Equivalent expression of  $F_2$  topological invariant using the non-abelian berry connection*, Phys. Rev. B **84**, 075119 (2011).
- [40] R. M. Fernandes and L. Fu, *Charge-4e superconductivity from multi-component nematic order*, Physical Review Letters **127**, 047001 (2021).
- [41] A. A. Golubov, M. Y. Kupriyanov, and E. Il'ichev, *The current-phase relation in josephson junctions*, Reviews of Modern Physics **76**, 411–469 (2004).
- [42] J. Clarke and A. I. Braginski, eds., *The SQUID Handbook: Fundamentals and Technology of SQUIDs and SQUID Systems* (Wiley–VCH, Weinheim, 2004).
- [43] D. Drung, C. Krause, U. Becker, H. Scherer, and F. J. Ahlers, *Ultrastable low-noise current amplifier: A novel device for measuring small electric currents with high accuracy*, Review of Scientific Instruments **86**, 024703 (2015).

# Supplemental Material for Quaternionic superconductivity with a single-field Bogoliubov-de Gennes–Ginzburg-Landau framework and charge-4e couplings

## S1. ANALYTIC DERIVATIONS: FLUCTUATION BUBBLE $\Pi(0)$ AND SECOND JOSEPHSON HARMONIC $J_2$

$$\mathbf{S1.1. Gaussian evaluation of } \Pi(0) = \int \frac{d^d \mathbf{k}}{(2\pi)^d} G_q^2(\mathbf{k})$$

Near  $T_c$  in the classical (static) GL regime, the quadratic action for the pair field  $q$  yields the propagator

$$G_q(\mathbf{k}) = \frac{1}{\alpha + \kappa k^2}, \quad (\text{S1})$$

with mass  $\alpha \propto (T - T_c)$  and stiffness  $\kappa > 0$ . The vestigial 4e channel acquires the one-loop correction

$$\Pi(0) = \int \frac{d^d \mathbf{k}}{(2\pi)^d} \frac{1}{(\alpha + \kappa k^2)^2}. \quad (\text{S2})$$

Rescaling  $k \mapsto k\sqrt{\kappa}$  and using the standard  $d$ -dimensional integral

$$\int \frac{d^d \mathbf{k}}{(2\pi)^d} \frac{1}{(k^2 + m^2)^n} = \frac{1}{(4\pi)^{d/2}} \frac{\Gamma(n - \frac{d}{2})}{\Gamma(n)} (m^2)^{\frac{d}{2} - n},$$

with  $n = 2$  and  $m^2 = \alpha/\kappa$ , we obtain

$$\Pi(0) = \frac{\Gamma(2 - \frac{d}{2})}{(4\pi)^{d/2}} \alpha^{\frac{d}{2} - 2} \kappa^{-\frac{d}{2}}. \quad (\text{S3})$$

For the experimentally relevant cases:

$$d = 2 : \quad \Pi(0) = \frac{1}{4\pi} \frac{1}{\alpha \kappa}, \quad (\text{S4a})$$

$$d = 3 : \quad \Pi(0) = \frac{1}{8\pi} \frac{1}{\kappa^{3/2} \alpha^{1/2}}. \quad (\text{S4b})$$

Thus, integrating out Gaussian  $q$  fluctuations renormalizes the quartet mass as

$$\mu_{\text{eff}} = \mu - g^2 \Pi(0), \quad (\text{S5})$$

and softens rapidly as  $T \rightarrow T_c^+$  according to Eqs. (S4). In quasi-2D films, the enhancement  $\Pi(0) \propto \alpha^{-1}$  makes a vestigial uniform 4e phase particularly accessible. A finite microscopic cutoff  $k_c \sim \xi_0^{-1}$  can be included by replacing  $\Pi(0)$  with  $\int^{k_c} d^d k (\alpha + \kappa k^2)^{-2}$ ; for  $d < 4$  the zero-cutoff results above are UV-convergent and universal.

*Remark on dynamics.* In the classical critical window the static ( $\omega_n = 0$ ) Matsubara sector dominates; dynamic corrections only renormalize prefactors.

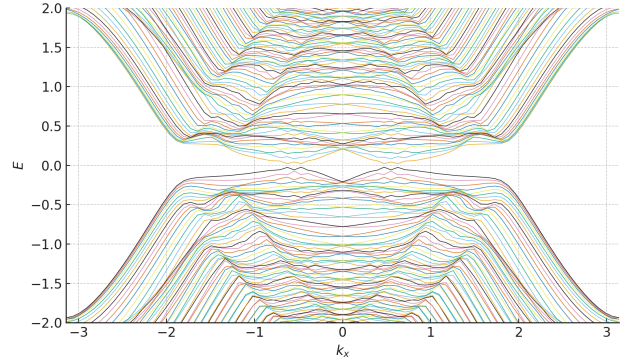


FIG. S1: Strip spectrum  $E(k_x)$  for the 2D class-DIII model (open along  $y$ ,  $N_y = 300$ ; parameters as in the main text). Bulk continua form the gapped bands; the two linear branches crossing at  $k_x \simeq 0$  are helical Majorana edge modes localized on opposite edges (Kramers partners at  $k_x = 0$ ). This matches the  $\mathbb{Z}_2$  index computed directly from  $q(\mathbf{k})$  in the main text.

## S1.2. Microscopic origin of the second Josephson harmonic $J_2$ from coherent 4e tunneling

Consider two conventional superconductors (phases  $\phi_L, \phi_R$ ) connected by a weak tunnel contact,

$$H = H_L + H_R + H_T, \quad (\text{S6})$$

$$H_T = \sum_{kp\sigma} (T_{kp} c_{Lk\sigma}^\dagger c_{Rp\sigma} + \text{h.c.}) \quad (\text{S7})$$

Integrating out fermions generates the effective phase action

$$S_{\text{eff}}[\phi] = -\text{Tr} \ln \left( 1 - \hat{\mathcal{T}} \hat{G}_L \hat{\mathcal{T}}^\dagger \hat{G}_R \right), \quad (\text{S8})$$

and expanding,

$$S_{\text{eff}} = \underbrace{\frac{1}{2} \text{Tr}[(\hat{\mathcal{T}} \hat{G}_L \hat{\mathcal{T}}^\dagger \hat{G}_R)^2]}_{\propto \cos \phi} + \underbrace{\frac{1}{4} \text{Tr}[(\hat{\mathcal{T}} \hat{G}_L \hat{\mathcal{T}}^\dagger \hat{G}_R)^4]}_{\propto \cos 2\phi} + \dots, \quad (\text{S9})$$

with  $\phi = \phi_L - \phi_R$ . The second-order term yields the standard  $-J_1 \cos \phi$  (Ambegaokar–Baratoff limit); the fourth order produces a *coherent two-Cooper-pair* process  $-J_2 \cos(2\phi)$ . Using anomalous Green functions in the tunneling limit and defining the dimensionless transparency  $\tau = \pi^2 N_L(0) N_R(0) |T|^2 \ll 1$ ,

$$J_1(T) = \frac{\pi \Delta}{2eR_N} \tanh \frac{\Delta}{2T} \quad (\text{identical leads}), \quad (\text{S10a})$$

$$J_2(T) \propto \tau^2 \frac{\Delta}{R_N^2} \mathcal{I}(T/\Delta), \quad (\text{S10b})$$

so that  $J_2/J_1 = \mathcal{O}(\tau)$  in the tunnel regime. The current–phase relation (CPR) is

$$I(\phi) = I_1 \sin \phi + I_2 \sin(2\phi) + \dots, \quad I_n = \frac{2e}{\hbar} n J_n. \quad (\text{S11})$$